CrossMark

Effect of Trisodium Citrate Concentration on the Structural and Photodiode Performance of CdO Thin Films

M. RAVIKUMAR,[1] S. VALANARASU,[2] R. CHANDRAMOHAN,[3]
S. SANTHOSH KUMAR JACOB,[2] and A. KATHALINGAM[4,5]

1.—Department of Physics, Arumugam Pillai Seethai Ammal College, Tiruppattur 630 211, India.
2.—PG and Research Department of Physics, Arul Anandar College, Karumathur 625514, India.
3.—Department of Physics, Sree Sevugan Annamalai College, Devakottai 630303, India.
4.—Millimeter-Wave Innovation Technology Research Center (MINT), Dongguk University, Seoul 100-715, Republic of Korea. 5.—e-mail: kathu@dgu.edu

CdO thin films were deposited on glass and silicon substrates by simple perfume atomizer at 350°C using cadmium acetate and trisodium citrate (TSC). The effect of the TSC concentration on the structural, morphological, optical, and photoconductive properties of the prepared CdO thin films was investigated. X-Ray diffraction (XRD) studies of the deposited films revealed improvement in crystalline nature with increase of TSC concentration. Films prepared without TSC showed porous nature, not fully covering the substrate, whereas films prepared using TSC exhibited full coverage of the substrate with uniform particles. Optical transmittance study of the films showed high transmittance (50% to 60%), and the absorption edge was found to shift towards the red region depending on the TSC concentration. The films exhibited a direct band-to-band transition with bandgap varying between 2.31 eV and 2.12 eV. Photoconductivity studies of the n-CdO/p-Si structure for various TSC concentrations were also carried out. I–V characteristics of this n-CdO/p-Si structure revealed the formation of rectifying junctions, and its photoconductivity was found to increase with the TSC concentration.

Key words: Perfume atomizer, CdO thin films, heterostructure, photodiode, electrical studies

INTRODUCTION

Cadmium oxide (CdO) is a promising material for various applications because of its properties similar to ZnO and TiO$_2$. Considerable attention has been paid to pure and metal-doped CdO thin films due to their wide range of applications in optoelectronics, such as transparent conducting oxide (TCO), solar cells, smart windows, optical communications, flat-panel displays, phototransistors, as well as other types of applications such as infrared (IR) heat mirrors, gas sensors, low-emissive windows, thin-film resistors, etc.[1–5] All these applications are based on the interesting optical and electrical properties of CdO. Pure CdO has n-type semiconducting behavior with high electrical conductivity (10^2 S/cm to 10^4 S/cm). Moreover, it is transparent in the visible and near-infrared (NIR) spectral regions with a direct bandgap of 2.2 eV to 2.7 eV.[1,6–8] To synthesize CdO thin films, several methods such as spray pyrolysis,[9] sputtering,[10] chemical bath deposition (CBD),[11] pulsed laser deposition,[12,13] metalorganic chemical vapor deposition (MOCVD),[1,14] sol–gel spin coating,[15] and spray pyrolysis using perfume atomizer[16] have been used. Among these methods, the perfume atomizer method has various advantages such as cost effectiveness, simplicity, ability to produce multicomponent oxide films on different substrates with various compositions, and allowing excellent compositional control and homogeneity. Also, spray parameters such as the spray rate, substrate temperature, spray nozzle distance, and solution concentration

can be used to tune the film properties well. The spray technique also has the advantage of tuning the properties of the thin films just by changing complexing agents (CA) in the precursor solution.[17] Many researchers therefore introduced CA, which control the metal ion concentration during the deposition process, to prepare uniform thin films.[18,19] In addition, the morphological properties of the thin-film layers are found to be strongly dependent on the appropriate CA.[20] Hydrazine hydrate (HH) plays a vital role as a side CA,[21] improving the growth rate and interfacial adherence of such thin films.[20,22] However, it suffers drawbacks in the form of its highly flammable, toxic, and carcinogenic nature. Therefore, considerable efforts have been made to replace HH with nontoxic CA such as disodium ethylenediamine tetraacetic acid (Na_2EDTA) and tartaric acid during the deposition process.[23,24] Although many thin films have been successfully deposited using the above-mentioned nontoxic CA, the deposited thin films indicated poor crystallinity, rough morphology, and discontinuous microstructures.[25] Use of citrate complexes is advantageous as citrate anions $(C_6H_5O_7)^{3-}$ with one to three carboxylate groups can be obtained, depending on the pH of the reaction solution.[26] Since citrate anions give three carboxylate groups, they can easily form strong complexes with Zn^{2+} ions and even Fe^{3+}, Cd^{2+}, Ag^+, and Mg^{2+} ions in basic pH solution.[26] Recently, use of Na_3-citrate as a CA has demonstrated the feasibility of improving the coverage of the absorber layer and creating a denser microstructure of ZnS thin film.[20,24] In the present work, we used a perfume atomizer to deposit CdO thin films using trisodium citrate as a CA. Hence, the effect of change of the trisodium citrate concentration on the structural, morphological, optical, and CdO/Si heterojunction photodiode properties was studied. To the best of our knowledge, deposition of CdO thin films by perfume atomizer using trisodium citrate (TSC) as complexing agent has not been reported yet.

EXPERIMENTAL PROCEDURES

CdO thin films were prepared by spray pyrolysis using a simple perfume atomizer. Cadmium acetate (0.1 M) with different volumes (0 mL, 1 mL, and 2 mL) of 0.1 M trisodium citrate was taken with deionized (DI) water as the spray solution. For each deposition, 50 mL solution was sprayed through a perfume bottle onto preheated (350°C) glass and p-Si substrates. Before the start of the deposition process, the glass plates were cleaned with chromic acid and acetone, then ultrasonically cleaned with deionized water to remove any contaminants on the surface and improve film adhesion. The experiment was repeated three times keeping the spray interval as 5 s. The thickness of the deposited films was measured by the weight difference method. After measuring the thickness, they were subjected to

morphological and optical studies using x-ray diffraction (XRD) analysis and scanning electron microscopy (SEM). XRD study was carried out using an X'Pert PRO (PANalytical) diffractometer with Cu K_x radiation ($k = 0.15405$ nm) in steps of $0.1°$ over the 2θ range from $15°$ to $75°$. A Hitachi S-3000H model SEM was used to study the particle size and morphology of the grown CdO thin films. For SEM studies, samples were coated with Au using a JFC-1100 model sputter instrument. Optical transmission study was also carried out using a PerkinElmer Lambda 35 spectrophotometer in the wavelength range from 350 nm to 850 nm. Films deposited on silicon substrates were coated with Al metal electrodes with thickness of about 250 nm using a metal mask in a thermal evaporator to study the photoresponse. A schematic of the fabricated n-CdO/p-Si device used for the photoresponse study is shown in the bottom right inset of Fig. 5. A 200-W halogen lamp was used for optical illumination of the device. A Keithley 4200 semiconductor parameter analyzer was used to record the photocurrent of the device.

RESULTS AND DISCUSSION

The presence of CA in the precursor solution resulted in smooth films with homogeneous distribution of grains compared with films deposited without CA. A similar observation has also been reported for preparation of CdTe films using ethylenediamine as CA in the spray pyrolysis method.[27] This implies that the film surface is dependent on the CA and its concentration. The thickness of the grown films was estimated by the weight gain method using the formula given in Eq. 1,

$$t = \frac{m}{A\rho},\tag{1}$$

where t is the thickness of the film, m is the weight gain measured by four-digit digital balance, A is the area of the coated film, and ρ is the density of the film (8.15 g/cm^3). The film thickness was found to increase with increasing CA volume from 0 mL to 2 mL. The estimated film thickness was found to be approximately 1.53 μm, 1.66 μm, and 1.94 μm for trisodium citrate volume of 0 mL, 1 mL, and 2 mL, respectively. This is attributed to the increase of the solution density with addition of trisodium citrate.

Structural Analysis

Figure 1 shows the XRD patterns of CdO thin films deposited using different volumes (0 mL, 1 mL, and 2 mL) of 0.1 M trisodium citrate CA. All the diffraction peaks in the XRD patterns could be indexed to the cubic crystal structure of CdO, in good agreement with the standard data for CdO [Joint Committee on Powder Diffraction Standards (JCPDS) data file no. 78-0653]. This is in accordance

with reports on CdO thin films prepared by the spray pyrolysis method.[28] The grown CdO exhibited strong orientation along (2 0 0) plane and also showed reflections along (1 1 1), (2 2 0), (3 1 1), and (2 2 2) planes too. It was found that the peak intensity increased as the concentration of trisodium citrate was increased, which is attributed to improvement of the crystalline nature of the film with increasing trisodium citrate concentration. Similar results were reported by Gadakh et al.[29] for Bi_2S_3 films with oxalic acid as CA. The average crystallite size of the samples was calculated using the well-known Scherrer formula

$$D = \frac{0.9\lambda}{\beta \cos \theta}, \qquad (2)$$

where β is the full-width at half-maximum (FWHM), θ is the Bragg angle, and λ is the x-ray wavelength used (1.5406 Å). The calculated crystallite size values are presented in Table I, showing that the crystallite size increased as the trisodium citrate concentration was increased. This may be due to improvement of the crystalline nature with increasing trisodium citrate concentration. This is because, with increased trisodium citrate concentration, there is a tendency for smaller crystallites to agglomerate into larger ones. From the calculated crystallite size values, the dislocation density and microstrain of the samples were also determined using Eqs. 3 and 4, respectively.

$$\delta = \frac{1}{D^2}, \qquad (3)$$

$$\varepsilon = \frac{\beta \cot \theta}{4}, \qquad (4)$$

where D is the crystallite size and β is the FWHM of the XRD peak. The calculated dislocation density and microstrain of the samples are also given in Table I. As the trisodium citrate concentration was increased, the values of δ and ε decreased. This is attributed to a decrease of defect levels and grain boundaries due to the increase of the crystallite size with the trisodium citrate concentration. This also indicates that decrease of lattice imperfections and improvement in film quality can be produced by the use of trisodium citrate as CA. No metallic cadmium phases were observed in the XRD patterns, hence these results reveal that the trisodium citrate concentration influenced the structural properties of the CdO films.

Morphological and Compositional Studies

The surface morphology of the CdO thin films was investigated by using scanning electron microscopy. Figure 2 shows SEM images of CdO films deposited onto glass substrates. The film prepared without using CA shows holes and voids with discontinuities
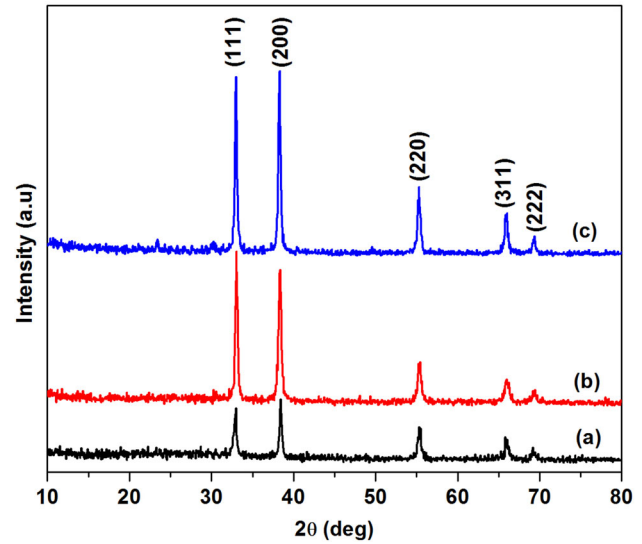

Fig. 1. XRD patterns of CdO thin-film samples prepared using (a) 0 mL, (b) 1.0 mL, and (c) 2.0 mL TSC.

on the surface of the substrate (Fig. 2a), whereas the films prepared with 1 mL CA were found to show improved morphology, fully covering the substrate with granular particles of nanosize (Fig. 2b). A slightly porous nature is shown, with uniformly distributed CdO particles. This reduced porosity of the film deposited using 1 mL of CA is probably due to the filled clusters of smaller nanograins. For 2 mL CA, the films showed denser and more uniform cauliflower-shaped grains of larger size compared with the other films (Fig. 2c). Here, trisodium citrate acted as a surfactant, allowing easy spreading of the solvent by lowering its surface tension.[30] Therefore, upon increasing the Na_3-citrate concentration, the resulting CdO thin films were found to consist of CdO clusters with smooth and denser microstructure compared with the film deposited without Na_3-citrate. When the CA concentration in the reaction bath was increased, all positively charged Cd^{2+} ions reacted with CA to form $Cd–[CA]^{2+}$, leading to a dominantly heterogeneous reaction on the substrate surface. Therefore, CdO thin film coated using high CA concentration exhibits dense microstructure, full coverage, and smooth and uniform morphology with improved crystalline quality.[31] This enlargement of the crystallite size for higher CA concentration was also evidenced by the XRD results. The EDAX spectrum taken for the CdO film deposited using 2 mL CA is shown in Fig. 2d, revealing the presence of Cd and O in the spray-deposited film.

Optical Studies

Figure 3 shows the optical transmittance spectra of the CdO films deposited using different volumes of trisodium citrate solution as observed in the wavelength range from 300 nm to 1200 nm. Variation of

Table I. Variation of crystallite size (D), dislocation density (δ), and microstrain (ε) of CdO thin films

S. No.	Trisodium citrate concentration (mL)	Crystallite size, D (nm)	Dislocation density, δ (10^{-4} lines m^{-2})	Microstrain, ε
1	0	41.32	5.857	7.723
2	1.0	49.87	4.021	6.399
3	2.0	65.72	2.315	4.854
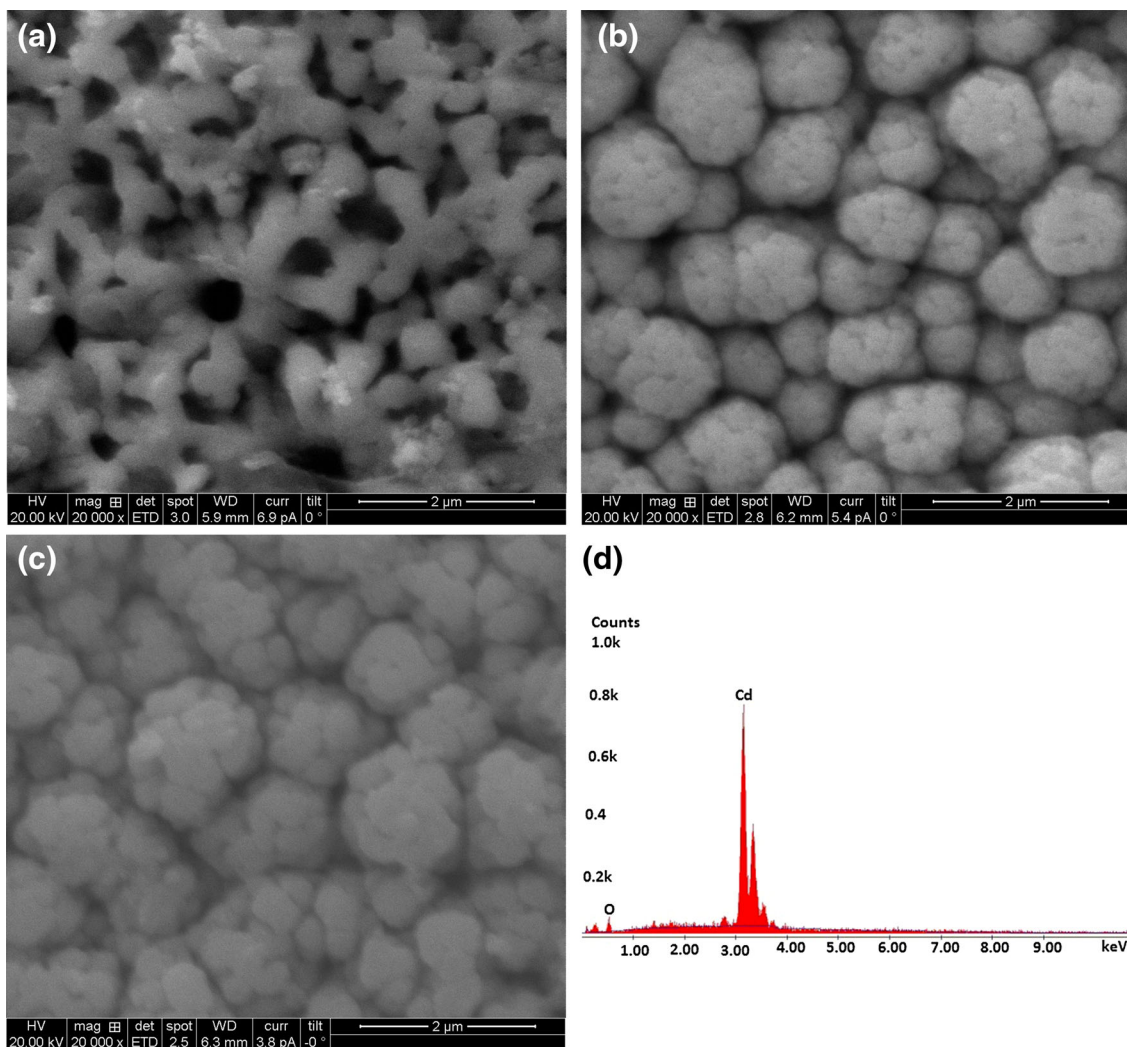
Fig. 2. SEM images of CdO thin films prepared with (a) 0 mL, (b) 1.0 mL, and (c) 2.0 mL TSC; (d) EDAX spectrum of CdO thin film prepared with 2.0 mL TSC.

the trisodium citrate concentration in the films markedly affected the optical properties of the grown films. Film coated without using CA showed high transmittance of 65%, and this value gradually decreased with increase of the trisodium citrate concentration in the spray solution. This transmittance reduction might be due to the increase in the film thickness with the trisodium citrate concentration. It is also noted that there is a slight shift of the optical absorption edge towards the red region as the

trisodium citrate concentration was increased, suggesting that there is a decrease in the optical bandgap (E_g). The sharp absorption edge obtained for all the films clearly shows their crystalline quality.

To determine the optical bandgap energy of the CdO films, the variation of the absorption coefficient (α) of the films with respect to thickness was obtained from the transmittance (T) values using Eq. 5 derived from Lambert's law, where t is the thickness and T is the transmittance of the films.
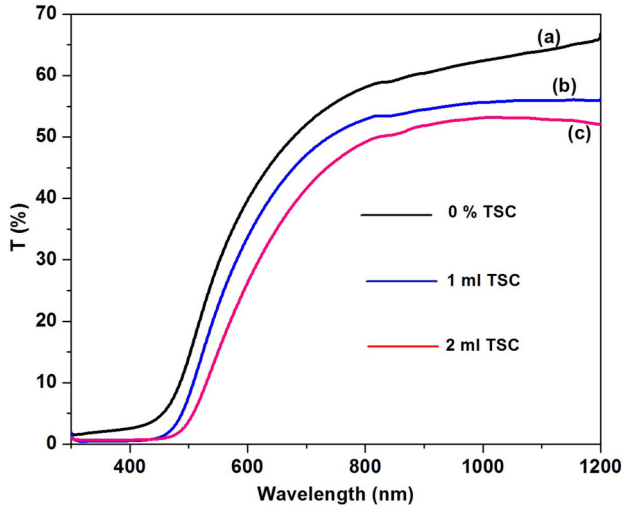
Fig. 3. Plots of transmittance (%) versus wavelength (nm) for CdO thin films prepared with (a) 0 mL, (b) 1.0 mL, and (c) 2.0 mL TSC.
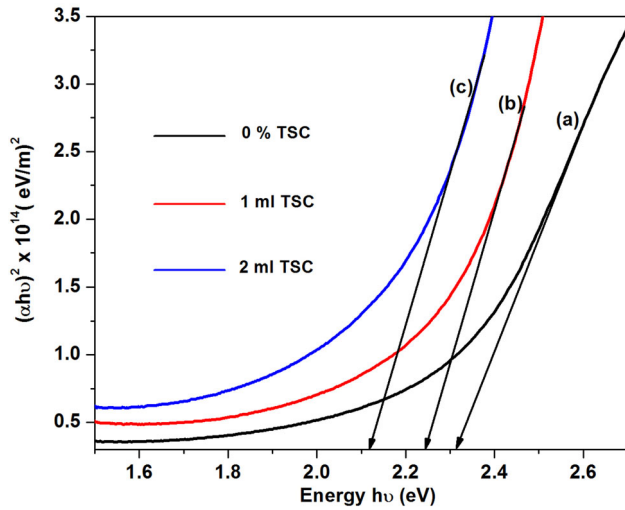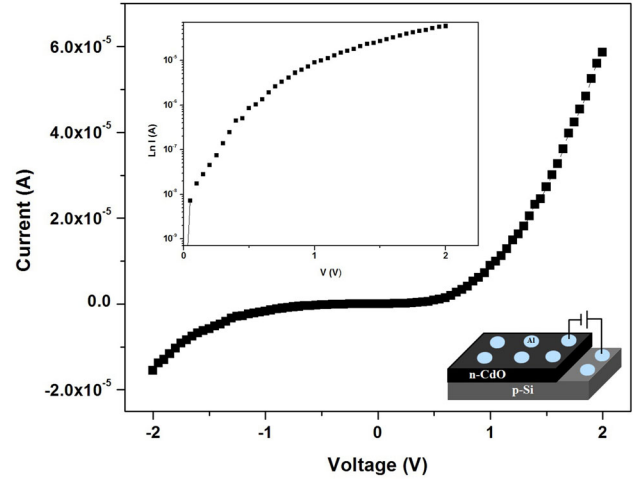

Fig. 5. Current–voltage characteristics of the *n*-CdO/*p*-Si heterojunction diode under dark conditions; insets: *top left* semilog plot of forward *I–V* curve, *bottom right* schematic view of the device.

Fig. 4. Plot of $(\alpha h v)^2$ (eV^2 cm^{-2}) versus photon energy (eV) for CdO thin films prepared with (a) 0 mL, (b) 1.0 mL, and (c) 2.0 mL TSC.

$$\alpha = \frac{I_n(1/T)}{t}. \qquad (5)$$

The bandgap of a material can be obtained from the absorption coefficient (α) using Eq. 6.

$$\alpha = A(hv - E_g)^{n/2}, \qquad (6)$$

where E_g is the bandgap, A is a constant, and n is a constant which is equal to 1 for a direct-gap material and 4 for an indirect-gap material. To determine whether the CdO films have a direct or indirect bandgap, $(\alpha h v)^2$ versus (hv) and $(\alpha h v)^{1/2}$ versus (hv) plots were drawn. Since better linearity was obtained in the $(\alpha h v)^2$ versus (hv) plot and also as it

is generally considered a direct-bandgap material,[32–34] the linear portion of the $(\alpha h v)^2$ versus (hv) plot was extrapolated to the energy axis (Fig. 4) to determine the bandgap value. The direct bandgap values obtained for the films were found to vary between 2.31 eV and 2.21 eV. Bandgap values of CdO thin films obtained by various methods have been found to lie in the range of 2.4 eV and 2.54 eV for sputtering, 2.3 eV and 2.5 eV for spray pyrolysis, 2.3 eV and 2.63 eV for CBD, and 2.42 eV for the sol–gel technique.[35–40] The bandgap values for CdO obtained in this work were found to be low compared with earlier works, which may be due to the increase of the crystallite size and thickness of the films for higher trisodium citrate concentrations. This indicates that the optical bandgap of CdO film can be controlled via the trisodium citrate concentration.

Photoresponse Study

The photoresponse of the films grown on *p*-silicon substrates was also studied using a 200-W halogen lamp as photoexcitation source. Figure 5 shows the *I–V* characteristics of the fabricated *n*-CdO/*p*-Si heterojunction diode in the forward and reverse directions under dark condition; the top left inset of this figure depicts a semilog plot of the forward response. The nonlinear, asymmetric nature of the *I–V* characteristic with low current in reverse and high current in forward bias indicates that the *n*-CdO/*p*-Si structure behaves as a rectifying heterojunction diode with rectification ratio of 5.5 at about 1 V and turn-on voltage of around 0.4 V. The current in the heterojunction device can be given by the relation[41–44]

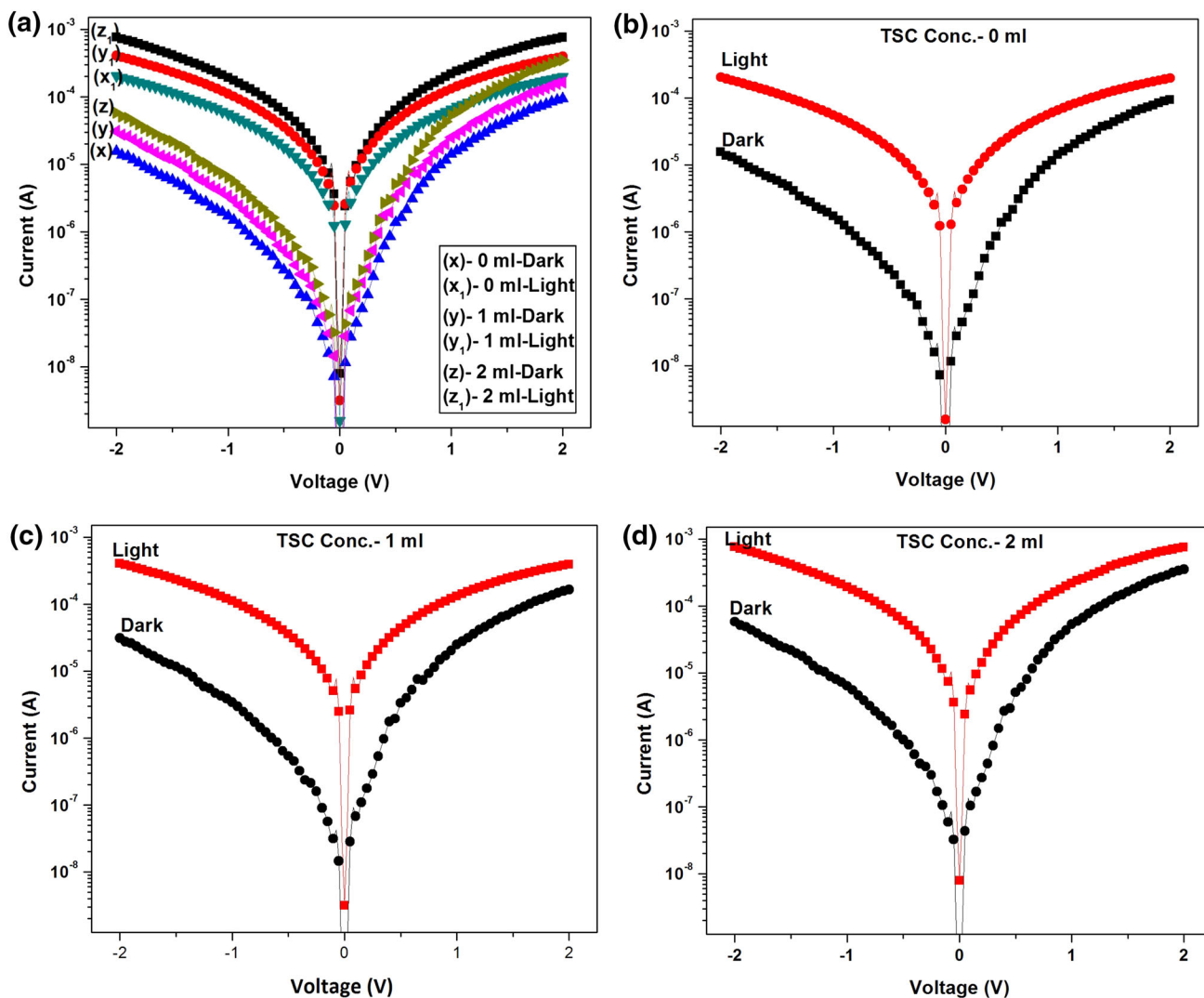$$I = I_s \exp\left(\frac{qV}{nkT} - 1\right), \qquad (7)$$

Fig. 6. Photoresponse *I–V* characteristics of *n*-CdO/*p*-Si heterojunction diodes for CdO thin films prepared with (a) all the films, and (b) 0 mL, (c) 1.0 mL, and (d) 2.0 mL TSC.

where q is the electronic charge, k is the Boltzmann constant, V is the applied voltage, I_s is the saturation current, n is the ideality factor of the device, and T is temperature. Under forward bias, i.e., greater than a few kT/q volts, Eq. 7 can be written as

$$I = I_s \exp\left(\frac{qV}{nkT}\right). \qquad (8)$$

Taking the log of Eq. 8 yields

$$\mathrm{Log}(I) = \log(I_s) + (q/nkT)V, \qquad (9)$$

where q/nkT is the slope of the *I–V* curve.

Hence, the ideality factor n can be obtained from the slope of the linear region of a forward-bias ln *I–V* plot. The room-temperature value of the ideality factor obtained for the *p*-CuO/*n*-Si

heterojunction was found to be 4.2 in the voltage range of 1 V to 2 V. This higher value of the ideality factor could be due to the presence of interface states, oxide layer on the silicon wafer, and series resistance. The *I–V* characteristics of the different *n*-CdO/*p*-Si heterojunction devices under dark and illumination conditions are shown in Fig. 5a–d. Figure 5a shows the relative changes of current obtained for all the devices fabricated using CdO films prepared with 0 mL, 1 mL, and 2 mL trisodium citrate CA in the spray solution. Figure 5b–d shows the results for individual devices under dark and illuminated conditions. All the devices showed approximately 10 times increased current under illumination than in the dark under reverse bias, whereas the increase was smaller under forward bias. Also, it was found that there was an increase of current in both dark and illuminated conditions with increase of the trisodium citrate complex concentration. This result indicates that increase of the

TSC molar concentration could increase the photo-sensing effect of this n-CdO/p-Si heterostructure. This increase may be due to the decrease of the energy bandgap value[45] because of the improved crystalline quality of the films and grain size. When the grain size is increased, charge transport is mainly intra-granular, which results in a substantial improvement in the electrical conductivity of the film. However, for smaller grains, the higher number of grain boundaries may act as low-conductivity blockades, increasing the resistivity. This study of the CdO-based heterostructure confirms that the n-CdO/p-Si structure can be used as a good photosensor (Fig. 6).

CONCLUSIONS

CdO thin films were successfully prepared on glass and p-Si substrates using the perfume atomizer method from aqueous solution containing trisodium citrate CA. n-CdO/p-Si heterojunction-based photodiodes were prepared and their photoresponse activity demonstrated. SEM and XRD studies of the grown CdO thin films revealed that the morphology and crystalline quality of the films could be improved by increasing addition of trisodium citrate CA. The bandgap value of the CdO thin films was found to vary from 2.31 eV to 2.21 eV with increasing TSC concentration. The prepared n-CdO/p-Si heterostructure diodes exhibited good rectifying behavior with ideality factor of 4.2 and rectification ratio of 5.5 at 1 V. Thus, the reported results could act as great motivation for further work to improve the properties of such photodiodes for application in optoelectronic devices.

REFERENCES

1. Z. Zhao, D.L. Morel, and C.S. Ferekides, *Thin Solid Films* 413, 203 (2002).
2. R. Rajammal, V. Anbarasu, E. Savarimuthu, and S. Arumugam, *J. Electron. Mater.* 43, 3514 (2013).
3. O. Gomez Daza, A. Arias-Carbajal Readigos, J. Campos, M.T.S. Nair, and P.K. Nair, *Mod. Phys. Lett. B* 17, 609 (2001).
4. A.A. Dakhel, *J. Electron. Mater.* 41, 2405 (2012).
5. M. Yan, M. Lane, C.R. Kannewurf, and R.P.H. Chang, *Appl. Phys. Lett.* 78, 02342 (2001).
6. D.M. Carballeda-Galicia, R. Castanedo-Perez, O. Jimenez-Sandoval, S. Jimenez-Sandoval, G. Torres-Delgado, and C.I. Zuniga-Romero, *Thin Solid Films* 371, 105 (2000).
7. K.L. Chopra and S. Ranjan Das, *Thin Film Solar Cells* (New York: Plenum, 1993).
8. Y.S. Choi, C.G. Lee, and S.M. Cho, *Thin Solid Films* 289, 0153 (1996).
9. P.M. Devshette, N.G. Deshpande, and G.K. Bichile, *J. Alloys Compd.* 463, 576 (2008).
10. Q. Zhou, Z. Ji, B. Hu, C. Chen, L. Zhao, and C. Wang, *Mater. Lett.* 61, 531 (2007).
11. M. Ortega, G. Santana, and A. Morales-Acevedo, *Solid State Electron.* 44, 1765 (2000).
12. B.J. Zheng, J.S. Lian, L. Zhao, and Q. Jiang, *Appl. Surf. Sci.* 256, 2910 (2010).
13. R.K. Gupta, K. Ghosh, R. Patel, S.R. Mishra, and P.K. Kahol, *Mater. Lett.* 62, 4103 (2008).
14. D. Lamb and S.J.C. Irvine, *Thin Solid Films* 518, 1222 (2009).
15. J. Santos-Cruz, G. Torres-Delgado, R. Castanedo-Perez, S. Jiménez-Sandoval, O. Jimenez-Sandoval, C.I. Zuniga-Romero, J. Marquez Marín, and O. Zelaya-Angel, *Thin Solid Films* 493, 83 (2005).
16. G. Shanmugavel, A.R. Balu, and V.S. Nagarethinam, *Int. J. Chem. Mater. Res.* 2, 88 (2014).
17. R. Gadakh and C.H. Bhosale, *Mater. Chem. Phys.* 64, 5 (2000).
18. T. Nakada, M. Hongo, and E. Hayashi, *Thin Solid Films* 431–432, 242 (2003).
19. S.D. Sartale, B.R. Sankapal, M. Lux-Steiner, and A. Ennaoui, *Thin Solid Films* 480, 168 (2005).
20. S.W. Shin, S.R. Kang, K.V. Gurav, J.H. Yun, J.H. Moon, J.Y. Lee, and J.H. Kim, *Sol. Energy* 85, 2903 (2011).
21. P.P. Hankare, P.A. Chate, D.J. Sathe, and A.A. Patil, *Appl. Surf. Sci.* 256, 81 (2009).
22. A. Antony, K.V. Murali, R. Manoj, and M.K. Jayaraj, *Mater. Chem. Phys.* 90, 106 (2005).
23. S.W. Shin, S.R. Kang, J.H. Yun, A.V. Moholkar, J.H. Moon, J.Y. Lee, and J.H. Kim, *Sol. Energy Mater. Sol. Cells* 95, 856 (2011).
24. A. Ennaoui, W. Eisele, M. Lux-Steiner, T.P. Niesen, and F. Karg, *Thin Solid Films* 431–432, 335 (2003).
25. I.L. Repins, B.J. Stanbery, D.L. Young, S.S. Li, W.K. Metzger, C.L. Perkins, W.N. Shafarman, M.E. Beck, L. Chen, V.K. Kapur, D. Tarrant, M.D. Gonzalez, D.G. Jensen, T. Anderson, X. Wang, L.L. Kerr, B. Keyes, S. Asher, A. Delahoy, and B. Von Roedern, *Prog. Photovolt. Res. Appl.* 14, 25 (2006).
26. S. Cho, J.W. Jang, S.H. Jung, B.R. Lee, E. Oh, and K.H. Lee, *Langmuir* 25, 3825 (2009).
27. K. Varasi Krishna, V. Dutta, 3rd World Conference on Photovoltaic Energy Conversion, Osaka, Japan 2003, 2P-A8-28.
28. R.J. Deokate, S.M. Pawar, A.V. Moholkar, V.S. Sawant, C.A. Pawar, C.H. Bhosale, and K.Y. Rajpure, *Appl. Surf. Sci.* 254, 2187 (2008).
29. S.R. Gadakh, V.V. Killedar, C.D. Lokhande, and C.H. Bhosale, *Mater. Chem. Phys.* 56, 79 (1998).
30. A.K. Thottoli and A.K.A. Unni, *J. Nanostruct. Chem.* 3, 56 (2013).
31. G.L. Agawane, S.W. Shin, A.V. Moholkar, K.V. Gurav, J.H. Yun, J.Y. Lee, and J.H. Kim, *J. Alloys Compd.* 535, 53 (2012).
32. S. Thangavel, S. Ganesan, and K. Saravanan, *Thin Solid Films* 520, 5206 (2012).
33. S.K. Vasheghani Farahani, V. Munoz-Sanjose, J. Zuniga-Perez, C.F. McConville, and T.D. Veal, *Appl. Phys. Lett.* 102, 022102 (2013).
34. C. Rajashree, A.R. Balu, and V.S. Nagarethinam, *J. Chem. Tech. Res.* 6, 347 (2014).
35. K. Gurumurugan, D. Mangalaraj, S.K. Narayandass, K. Sekar, and C.P. Girija Vallabhan, *Semicond. Sci. Technol.* 9, 1827 (1994).
36. T.L. Chu and S.S. Chu, *J. Electron. Mater.* 19, 1003 (1990).
37. C. Sravani, K.T.R. Reddy, P.S. Reddy, and P.J. JayaramaReddy, *Mater. Sci. Lett.* 13, 1045 (1994).
38. A.J. Varkey and A.F. Fort, *Thin Solid Films* 239, 211 (1994).
39. K. Gurumurugan, D. Mangalaraj, S.K. Narayandass, and C. Balasubramanian, *Phys. Status Solidi A* 143, 85 (1994).
40. M.Z. Najadoski, I. Grozdanov, and B. Minceva Sukarova, *J. Mater. Chem.* 65, 761 (1996).
41. S.M. Sze, *Physics of Semiconductor Devices*, Vol. 2 (New York: Wiley, 1981).
42. R.A. Ismail, A.-M.E. Al-Samarai, S.J. Mohmed, and H.H. Ahmed, *Solid-State Electron.* 82, 115 (2013).
43. M. Caglar and F. Yakuphanoglu, *J. Phys. D Appl. Phys.* 42, 045102 (2009).
44. S. Aksoy and Y. Caglar, *Eng. Technol.* 5, 11 (2011).
45. S. Jung, S. Ahn, J. Yun, J. Gwak, D. Kim, and K. Yoon, *Curr. Appl. Phys.* 10, 990 (2010).